AD_____

Award Number: DAMD17-99-1-9144

TITLE: Optimization of Technique Factors for Full-Field Digital Mammography and Comparison of Optimized Techniques to Screen-Film Mammography

PRINCIPAL INVESTIGATOR: Eric A. Berns
R. Edward Hendrick, Ph.D.

CONTRACTING ORGANIZATION: Northwestern University
Evanston, Illinois 60208-1110

REPORT DATE: September 2002

TYPE OF REPORT: Annual Summary

PREPARED FOR: U.S. Army Medical Research and Materiel Command
Fort Detrick, Maryland 21702-5012

REPORT DOCUMENTATION PAGE

Form Approved
OMB No. 074-0188

1. AGENCY USE ONLY (Leave blank)	2. REPORT DATE	3. REPORT TYPE AND DATES COVERED
	September 2002	Annual Summary (1 Feb 01 - 19 Aug 02)

4. TITLE AND SUBTITLE
Optimization of Technique Factors for Full-Field Digital Mammography and Comparison of Optimized Techniques to Screen-Film Mammography

5. FUNDING NUMBERS
DAMD17-99-1-9144

6. AUTHOR(S) :
Eric A. Berns
R. Edward Hendrick, Ph.D.

7. PERFORMING ORGANIZATION NAME(S) AND ADDRESS(ES)
Northwestern University
Evanston, Illinois 60208-1110

E-Mail: eberns@radiology.nwu.edu

8. PERFORMING ORGANIZATION REPORT NUMBER

9. SPONSORING / MONITORING AGENCY NAME(S) AND ADDRESS(ES)
U.S. Army Medical Research and Materiel Command
Fort Detrick, Maryland 21702-5012

10. SPONSORING / MONITORING AGENCY REPORT NUMBER

11. SUPPLEMENTARY NOTES

12a. DISTRIBUTION / AVAILABILITY STATEMENT
Approved for Public Release; Distribution Unlimited

12b. DISTRIBUTION CODE

13. ABSTRACT ***(Maximum 200 Words)***

The technical objectives of this study are to determine optimum techniques for a flat-panel Cesium-iodide silicon-diode full-field digital mammography system and to compare those optimized techniques to screen-film mammography at equal breast doses.

This project continued in the second year with work focused on analyzing the data and writing a manuscript for publication. Statistical analysis was performed using the SAS software package comparing contrast-detail scores and looking for trends among different target-filter combinations as kilo-voltage peak values were increased. From this, a manuscript was written titled "Optimization of technique factors for a silicon diode array full-field digital mammography system and comparison to screen-film mammography with matched average glandular dose". This paper represents presents the majority of results from this project to date. The paper was accepted for publication in Medical Physics for March 2003.

14. SUBJECT TERMS:
digital mammography, screen film mammography

15. NUMBER OF PAGES
13

16. PRICE CODE

17. SECURITY CLASSIFICATION OF REPORT	18. SECURITY CLASSIFICATION OF THIS PAGE	19. SECURITY CLASSIFICATION OF ABSTRACT	20. LIMITATION OF ABSTRACT
Unclassified	Unclassified	Unclassified	Unlimited

Table of Contents

Annual Summary Report

Award Number: DAMD17 – 99-1-9144

PI: R. Edward Hendrick, Ph.D. - Mentor
Eric A. Berns, M.S. – Pre-Doctoral Trainee

Report Date: 1-30-2003

Introduction

The replacement of screen-film image receptors by full-field digital image receptors may increase the visibility of lesions, especially those within glandular tissues, by decoupling image acquisition and image display. With digital mammography, there should be no loss of contrast within fibroglandular tissues. The effects of the characteristic curve of screen-film systems are eliminated and similar contrast resolution should exist among all breast tissues. Digital mammography systems permit user-adjustment of image display to maximize contrast resolution within specific tissues of interest. Thus, digital mammography has the potential to increase lesion visibility, especially improving the visibility of lesions in dense breasts, and the potential to decrease errors of perception and interpretation, again especially in dense breasts.

This projects will optimize techniques to improve the detection and diagnosis of breast cancer using full-field digital mammography and compare them to screen-film mammography. If our hypotheses are correct, this study will result in optimized clinical techniques for mammography sites and provide a solution for an important and difficult area for current mammography: lesion detection in thicker, denser breasts. Finally, this study should provide and answer to the question of how digital mammography compares to screen-film mammography in the detection of breast lesions.

Description of training and research accomplishments

This project continued in the second year with work focused on analyzing the data and writing a manuscript for publication. Statistical analysis was performed using the SAS software package comparing contrast-detail scores and looking for trends among different target-filter combinations as kilo-voltage peak values were increased. From this, a manuscript was written titled "Optimization of technique factors for a silicon diode array full-field digital mammography system and comparison to screen-film mammography with matched average glandular dose" (see appendix A). This paper represents a significant amount of work and presents the majority of results from this project to date. The paper was accepted for publication in Medical Physics for March 2003.

What remains to be done is to find optimized technique factors for different breast compositions at different breast thicknesses for digital mammography. Then, to compare these results to screen-film and the already measured fifty percent fat/fifty percent glandular breast composition data already collected.

Key Accomplishments

- Statistical analysis
- A manuscript

List of Reportable Outcomes

- Manuscript written and submitted for publication to Medical Physics titled "Optimization of technique factors for a silicon diode array full-field digital mammography system and comparison to screen-film mammography with matched average glandular dose". The manuscript was accepted for publication for the March 2003 issue. See appendix A.

Appendix A

Optimization of technique factors for a silicon diode array full-field digital mammography system and comparison to screen-film mammography with matched average glandular dose

Eric A. Berns[a] and R. Edward Hendrick
The Lynn Sage Comprehensive Breast Center, Northwestern University Medical School, Chicago, Illinois 60611

Gary R. Cutter
Center for Research Design and Statistical Methods, University of Nevada, Reno, Nevada

(Received 14 May 2002; accepted for publication 16 December 2002)

Contrast-detail experiments were performed to optimize technique factors for the detection of low-contrast lesions using a silicon diode array full-field digital mammography (FFDM) system under the conditions of a matched average glandular dose (AGD) for different techniques. Optimization was performed for compressed breast thickness from 2 to 8 cm. FFDM results were compared to screen-film mammography (SFM) at each breast thickness. Four contrast-detail (CD) images were acquired on a SFM unit with optimal techniques at 2, 4, 6, and 8 cm breast thicknesses. The AGD for each breast thickness was calculated based on half-value layer (HVL) and entrance exposure measurements on the SFM unit. A computer algorithm was developed and used to determine FFDM beam current (mAs) that matched AGD between FFDM and SFM at each thickness, while varying target, filter, and peak kilovoltage (kVp) across the full range available for the FFDM unit. CD images were then acquired on FFDM for kVp values from 23–35 for a molybdenum–molybdenum (Mo–Mo), 23–40 for a molybdenum–rhodium (Mo–Rh), and 25–49 for a rhodium–rhodium (Rh–Rh) target filter under the constraint of matching the AGD from screen film for each breast thickness (2, 4, 6, and 8 cm). CD images were scored independently for SFM and each FFDM technique by six readers. CD scores were analyzed to assess trends as a function of target–filter and kVp and were compared to SFM at each breast thickness. For 2 cm thick breasts, optimal FFDM CD scores occurred at the lowest possible kVp setting for each target–filter, with significant decreases in FFDM CD scores as kVp was increased under the constraint of matched AGD. For 2 cm breasts, optimal FFDM CD scores were not significantly different from SFM CD scores. For 4–8 cm breasts, optimum FFDM CD scores were superior to SFM CD scores. For 4 cm breasts, FFDM CD scores decreased as kVp increased for each target–filter combination. For 6 cm breasts, CD scores decreased slightly as kVp increased for Mo–Mo, but did not change significantly as a function of kVp for either Mo–Rh or Rh–Rh. For 8 cm breasts, Rh/Rh FFDM CD scores were superior to other target–filter combinations and increased significantly as kVp increased. These results indicate that low-contrast lesion detection was optimized for FFDM by using a softer x-ray beam for thin breasts and a harder x-ray beam for thick breasts, when AGD was kept constant for a given breast thickness. Under this constraint, optimum low-contrast lesion detection with FFDM was superior to that for SFM for all but the thinnest breasts. [DOI: 10.1118/1.1544674]

I. INTRODUCTION

Screening mammography trials have shown that mammography has a sensitivity to breast cancer ranging from 60% to 90%, with a trend toward lower sensitivity in premenopausal women.[1,2] Several independent analyses have shown that missed breast cancers are more likely to occur in radiographically dense breasts.[3–5] It is known that radiographically denser breasts have a greater probability of masking breast cancers, due to the similar x-ray attenuation properties of glandular tissues and breast cancers. The higher the glandular content of the breast, the greater the probability that breast cancer will be obscured by fibroglandular tissues.

The replacement of screen-film image receptors by full-field digital image receptors may increase the visibility of lesions, especially those within glandular tissues, by decoupling image acquisition and image display. Digital mammography eliminates the adverse effects of the characteristic curve, which reduces contrast in underexposed or overexposed screen-film images. Thus, in digital mammography adequate contrast resolution should exist among all breast tissues, as long as signal-to-noise ratios are adequate, since digital mammography permits user adjustment of image display to maximize contrast resolution within specific tissues of interest. Thus, digital mammography has the potential to increase lesion visibility, especially improving the visibility of lesions in dense breasts, and the potential to decrease errors of perception and interpretation. Preliminary studies of small-field and prototype full-field digital image receptors using contrast-detail phantoms suggest that digital mam-

PROOF COPY 020303MPH

mography will offer improved low-contrast resolution capabilities.[6]

There have been only a few published studies evaluating the influence of technique factors on low-contrast lesion detection with full-field digital mammography. Previous work has been done using an energy transport model to optimize spectral shape for a digital detector using a Gd_2O_2S scintillating screen coupled to a solid state CCD photodetector.[7] That work found that improvements in signal-to-noise ratios can be made by choosing different target materials for different breast thicknesses. Another study evaluated optimized technique parameters for a slot-scanning digital mammography system and suggested that optimization can maximize image quality and that each system be individually optimized.[8] Dance *et al.*, used measured spectra and Monte Carlo simulations to determine the effect of target–filter and tube potential on contrast, signal-to-noise ratios, and average absorbed doses in both screen-film and generic digital mammography.[9] Huda *et al.* modeled signal-to-noise ratios and breast dose as a function of photon energy in mammography using a figure of merit and assuming a monoenergetic x-ray beam.[10] The results of these previous studies are relevant to our study, but measurements were made on different detector types or simulations were made for more generic digital systems, not for the cesium-iodide silicon diode array used in this study.

Williams *et al.* evaluated the cesium-iodide amorphous silicon detector, along with two other digital mammography detectors, by using a "figure of merit" (FOM) as a metric for image quality.[11] In their work, FOM was defined as $FOM = SNR^2/AGD$, where AGD is the average glandular breast dose. Another metric used in the work was to measure the contrast-to-noise ratio across a slab of glandular tissue and calcified tissue relative to a uniform background. These measurements were taken for 3, 5, and 7 cm thick tissue-equivalent phantoms under manual exposures under the condition of an approximately matched detector signal.

In this paper, we determined optimized technique factors for the detection of low-contrast lesions using a silicon diode array full-field digital mammography (FFDM) system. FFDM AGD was matched to the AGD for screen-film mammography at each of four breast thicknesses: 2, 4, 6, and 8 cm. Then, as the target–filter and kVp were varied, FFDM AGD was kept constant for a given breast thickness. We compared FFDM results to screen-film mammography (SFM) results for low-contrast detection at each breast thickness. This paper differs from the previously cited paper by using the detection of simulated low-contrast lesions as the detection task and we perform this task under the condition of matched AGD to the breast, not matched signal to the detector.[11]

II. MATERIALS AND METHODS

Four contrast-detail (CD) images were acquired at 2, 4, 6, and 8 cm breast thicknesses on a SFM unit with optimized techniques using the optimization method described by Hendrick *et al.*, with target optical densities in the range of 1.55–1.70.[12] A D-shaped uniform CD phantom made of 1 cm slabs of tissue-equivalent material was used, one section of which contained a 9×9 contrast-detail pattern for the assessment of simulated low-contrast lesions (Fig. 1). The contrast-detail phantom was made from tissue-equivalent material designed to simulate 50% glandular/50% fatty breast tissues (BR 50/50). The phantom was the prototype for a digital mammography phantom offered commercially (Model 082, Computerized Imaging Reference Systems, Inc.), but has slightly different contrast specifications. Contrast was produced by circular holes drilled into the BR 50/50 breast equivalent material at diameters of 0.25, 0.5, 0.75, 1.0, 1.5, 2.0, 2.5, 3.0, and 4.0 mm. Each hole diameter was drilled at nine different depths of 0.05, 0.1, 0.15, 0.2, 0.3, 0.4, 0.5, 0.6, and 0.7 mm, yielding a square array of 81 objects. Each D-shaped slab was a semicircular phantom 18 cm in diameter and 1 cm thick. One D-shaped slab contained the contrast-detail pattern; the remainder were identical in shape but of uniform thickness and composition.

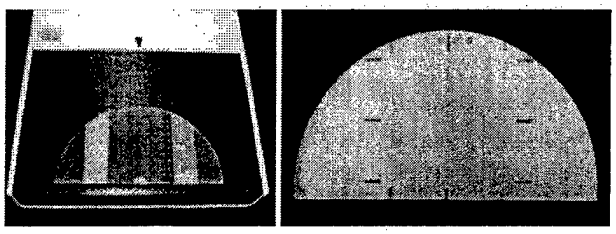

FIG. 1. Contrast-detail phantom on image receptor (left) and an x-ray image of the contrast-detail phantom (right).

Technique factors were recorded for each CD image and the corresponding AGD was calculated for each phantom thickness using HVL and entrance exposure measurements made on the SFM unit.[13,14]

To calculate techniques for the FFDM unit, a computer program was developed to determine the mAs value that gave an equal average glandular dose at each target–filter and kVp combination for each breast thickness. Half-value layer (HVL) and entrance exposure measurements were made on both the SFM unit and the FFDM unit at each target–filter and kVp to calculate AGD. The computer program was written to take into account any change in system performance (output or beam quality) and calculate the exact techniques needed to produce the desired average glandular dose.

CD images were then acquired on the FFDM unit using manual techniques for kVp values from 23–35 for Mo–Mo, 23–40 kVp for Mo–Rh, and 25–49 kVp for Rh–Rh, under the constraint of keeping AGD constant for a given breast thickness. mAs values were chosen to provide the matched AGD and images were acquired at approximately every second or third kVp step on the FFDM unit.

Screen-film CD images were scored by six readers under standardized viewing conditions. These included complete masking of each CD image and low ambient room lighting (<10 lux). Scoring of the CD phantom was done in a standardized manner, starting with the highest-contrast row of

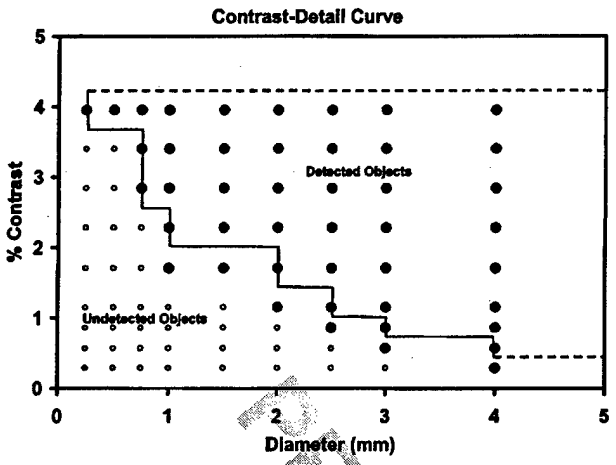

FIG. 2. Schematic of contrast-detail area score calculation. The CD score was defined as the product of the percent contrast and diameter area, including all detected objects.

objects, reading from the largest to smallest detectable object diameter in that row. An object was judged as "detected" if it occurred in the correct location, appeared generally round, and was more visible than artifactual "objects" occurring in the background of the CD phantom, excluding the locations of the 81 test objects. This comparison of detected objects against artifacts in the background of the phantom, similar to the method developed for scoring the ACR mammography accreditation phantom, was used to guard against overscoring due to prior knowledge of the location of the test objects in the phantom. Once an object was deemed too faint to detect, was not generally round, or was less conspicuous than artifacts in the background of the phantom, counting was stopped and the number of consecutively visible objects in that row was recorded. The reviewer then moved on to the next row of objects at slightly lower contrast, repeating the procedure. The CD score of each image was determined by calculating the area of detected objects in CD space (Fig. 2). The more low-contrast objects detected, the higher the CD score. If no objects were detected, a minimum score of zero would result; if all 81 objects were detected, a maximum score of 17.34 would result.

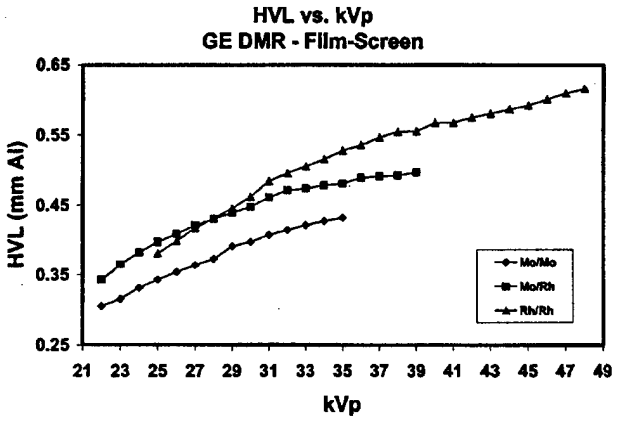

FIG. 3. HVL vs kVp results for the GE DMR screen-film unit.

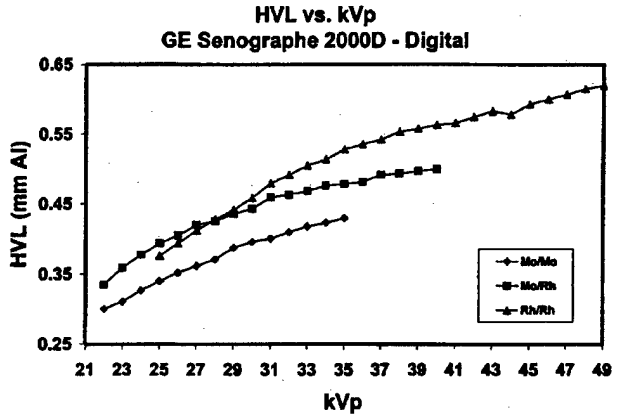

FIG. 4. HVL vs kVp results for the GE Senographe 2000D full-field digital mammography unit.

FFDM CD images were scored by the same six readers on the GE Review Workstation under optimized viewing conditions using the same scoring methods described above. Results were analyzed for statistical significance using analysis of variance methods (SAS Institute, Seattle, WA). CD scores were analyzed to assess trends as a function of target–filter and kVp using the general linear model (PROC GLM). Two-sided t tests were used to compare FFDM to SFM at each breast thickness (PROC T-TEST).[15]

III. RESULTS

Results of HVL measurements for the dose matching computer program are shown in Figs. 3 and 4 for both the GE DMR SFM unit and the GE Senographe 2000D FFDM unit. As expected, measured HVLs increased as kVp increased for each target–filter combination. HVL measurements were consistent between the SFM unit and FFDM unit, with HVL's ranging from 0.30 to 0.43 mm Al for Mo/Mo, 0.34 to 0.50 for Mo/Rh, and 0.38 to 0.62 for Rh/Rh.

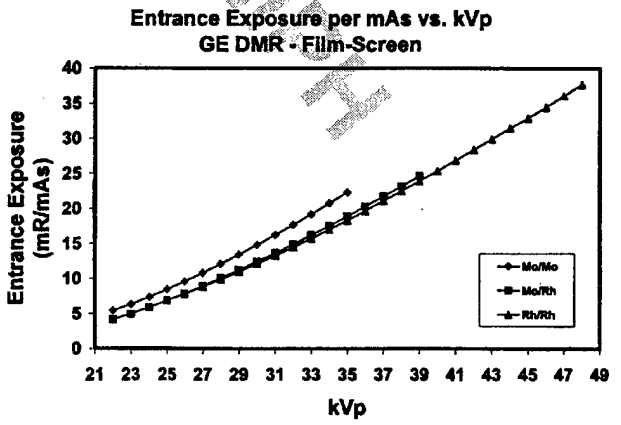

FIG. 5. Exposure output versus kVp results for the GE DMR screen-film unit.

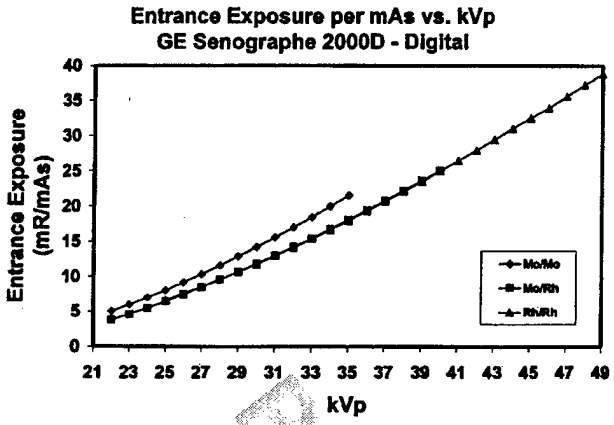

FIG. 6. Exposure output versus kVp results for the GE Senographe 2000D full field digital mammography unit.

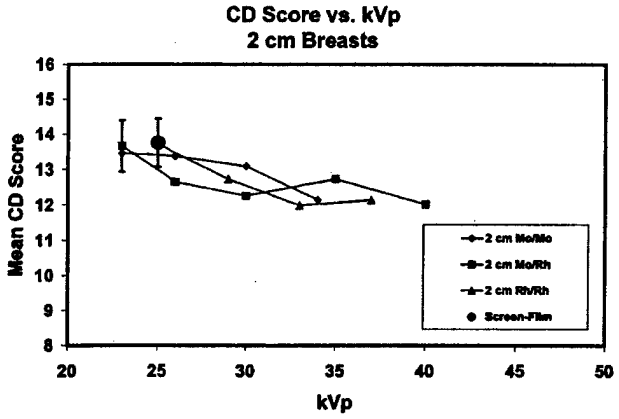

FIG. 7. CD score versus kVp for 2 cm breast thickness. The circular data point and error bars surrounding it represent the mean SFM CD score and plus and minus one standard deviation. The error bar on the highest FFDM CD score represents the mean plus and minus one standard deviation for all FFDM CD scores at this breast thickness.

Results of exposure output measurements used in the dose matching program are shown in Figs. 5 and 6 for both the GE DMR SFM unit and the GE Senographe 2000D FFDM unit. As expected, output in exposure per mAs rose as kVp increased for each target–filter combination. Output measurements were approximately consistent between the SFM unit and FFDM unit ranging from 5.0 to 22.4 mR/mAs ($1\ \text{mR} = 2.58 \times 10^{-7}\ \text{C/kg}$) for Mo/Mo, 3.8–25.0 mR/mAs for Mo/Rh, and 6.6–38.8 mR/mAs for Rh/Rh across the range of kVp values.

Results of contrast-detail imaging on the screen-film unit at 2, 4, 6, and 8 cm breast thicknesses are listed in Table I. All images had optical densities between 1.56 and 1.66, within the desired OD range for optimal detection of low-contrast lesions.[12]

Results of contrast-detail score measurements on screen-film and digital units with different target–filter and kVp combinations can be seen in Figs. 7–10. Figure 7 shows contrast-detail results of imaging a 2 cm thick breast. For the digital mammography system, the highest CD score occurred at the lowest possible kVp setting for each target–filter combination. The optimum digital mammography CD score for each of the three target–filters (13.45–13.71) was virtually identical to the optimized screen-film CD score (13.75) for 2 cm thick breasts. The significance of trends in CD scores values versus kVp is discussed at the end of this section.

TABLE I. Optimal screen-film techniques with HVL, average glandular dose, and optical density results.

	Optimized screen-film techniques and data			
	2 cm	4 cm	6 cm	8 cm
Target/filter	Mo/Mo	Mo/Mo	Mo/Rh	Rh/Rh
kVp	25	25	27	28
mAs	16	85	168	283
HVL (mm Al)	0.349	0.349	0.421	0.432
Average glandular dose (mGy)	0.39	1.26	2.35	3.85
Optical density	1.56	1.66	1.58	1.59

Figure 8 shows CD results for 4 cm thick breasts using both SFM and FFDM. Most FFDM CD scores exceeded the screen-film CD score for 4 cm thick breasts. Figure 9 shows that for 6 cm thick breasts, all FFDM CD scores exceeded the optimized screen-film CD score. Figure 10 shows that for 8 cm thick breasts, FFDM CD scores using Mo–Rh and Rh–Rh target–filters were superior to those for SFM. The highest CD scores for digital occurred with Rh–Rh, regardless of the kVp selected.

Optimal digital CD scores are compared to those for SFM in Table II. For 2 cm thick breasts, there was no statistical distinction between SFM and optimum FFDM CD scores. For 4 cm breasts, optimal FFDM CD scores occurred at 24 kVp for Mo–Mo (14.20), 35 kVp for Mo–Rh (14.38), and 29 kVp for Rh–Rh (14.36). The optimal FFDM CD score for each target–filter was superior to the SFM CD score ($p \leq 0.013$). For 6 cm breasts, optimum FFDM CD score oc-

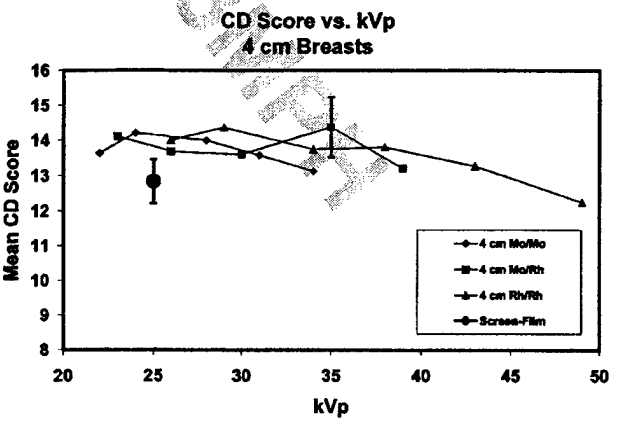

FIG. 8. CD score versus kVp for 4 cm breast thickness. The circular data point and error bars surrounding it represent the mean SFM CD score and plus and minus one standard deviation. The error bar on the highest FFDM CD score represents the mean plus and minus one standard deviation for all FFDM CD scores at this breast thickness.

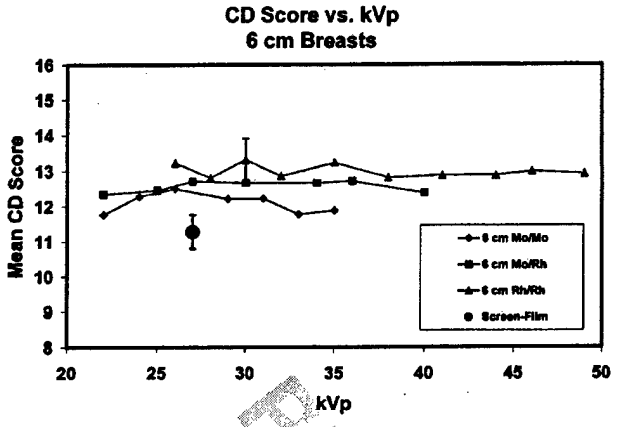

FIG. 9. CD score versus kVp for 6 cm breast thickness. The circular data point and error bars surrounding it represent the mean SFM CD score and plus and minus one standard deviation. The error bar on the highest FFDM CD score represents the mean plus and minus one standard deviation for all FFDM CD scores at this breast thickness.

cured for Rh–Rh at 30 kVp and was significantly higher than the SFM CD score (13.3 vs. 11.3, $p<0.0001$). In fact, for 6 cm thick breasts, all FFDM CD scores were higher than the SFM CD score (Fig. 9). For 8 cm breasts, optimum FFDM CD scores occurred for Rh–Rh at 46 kVp and were significantly higher than SFM CD scores (12.9 vs. 9.48, $p<0.0001$). In general, CD scores for Rh–Rh were higher than those for Mo–Mo or Mo–Rh at this breast thickness.

Trends in CD scores versus kVp at each breast thickness and target–filter combination are shown in Table III. Table III indicates that for 2 cm breasts, CD scores tended to drop as kVp increased for each target–filter material, but the trend was not statistically significant. For 4 cm breasts, CD scores also tended to drop as kVp increased; the trend was statistically significant, however, only for the Rh–Rh target–filter combination ($p=0.012$). For 6 cm thick breasts, no statistically significant trend in CD scores occurred for any target–filter combination. For 8 cm thick breasts, FFDM CD scores increased significantly as kVp increased for Mo–Mo and Rh–Rh target–filter combinations ($p<0.05$).

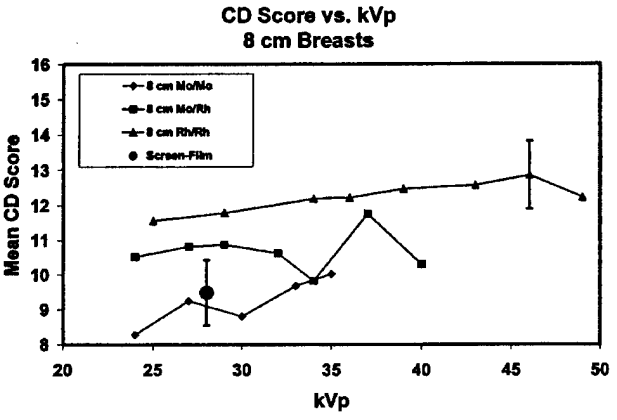

FIG. 10. CD score versus kVp for 8 cm breast thickness. The circular data point and error bars surrounding it represent the mean SFM CD score and plus and minus one standard deviation. The error bar on the highest FFDM CD score represents the mean plus and minus one standard deviation for all FFDM CD scores at this breast thickness.

TABLE II. Mean CD score comparison between screen-film and optimized digital techniques.

Mean CD score comparison underoptimized techniques			
Breast thickness	Screen-film Mean CD score	Optimal digital Mean CD score	*P* value
2 cm	13.8	13.5	0.47
4 cm	12.8	14.4	0.013
6 cm	11.3	13.3	<0.0001
8 cm	9.5	12.9	<0.0001

IV. DISCUSSION

Low-contrast detection in screen-film mammography was shown to be optimized by selecting Mo–Mo target–filter combinations for thin to intermediate breasts (under 5 cm) and by selecting Rh–Rh for thick breasts (over 7 cm).[10–12] With those target–filters, low-contrast detection was shown to be maximized by picking the lowest kVp that kept exposure times adequately short (under 2 s) for a given breast thickness.[12,16]

It might be expected that the optimization of technique factors in digital mammography would follow similar rules. The use of cesium-iodide as the scintillation material in digital mammography, however, instead of the gadolinium oxysulfide scintillator used in screen-film cassettes, complicates the issue. The two materials have different x-ray attenuation properties and different energy dependences of attenuation properties. In screen-film mammography, screens are required to be relatively thin to minimize blur. This, in turn, requires lower beam quality to achieve increased x-ray absorption. The linear structure of CsI crystals used as the scintillator in digital mammography reduces blur, so the CsI scintillator layer can be thicker, reducing the need for lower

TABLE III. Statistical significance of trends in CD scores versus kVp at each breast thickness and target–filter combination. The *r*-square value refers to the Pearson correlation coefficient obtained when a linear fit was performed on CD score versus kVp. The *p* value refers to the significance of the trend in CD score versus kVp.

Trend results for contrast-detail scores versus kVp				
Breast thickness	Target/filter	Mean value	*R* square	Trend *p* value
2 cm	Mo/Mo	13.0	0.855	0.075
	Mo/Rh	12.7	0.576	0.137
	Rh/Rh	12.6	0.813	0.099
4 cm	Mo/Mo	13.7	0.440	0.222
	Mo/Rh	13.8	0.119	0.569
	Rh/Rh	13.6	0.824	0.012
6 cm	Mo/Mo	12.1	0.068	0.571
	Mo/Rh	12.6	0.045	0.650
	Rh/Rh	13.0	0.147	0.274
8 cm	Mo/Mo	9.21	0.793	0.043
	Mo/Rh	10.7	0.001	0.945
	Rh/Rh	12.2	0.677	0.012

beam quality as a means to get increased absorption. The higher beam quality used in digital also increases x-ray output, thereby reducing exposure time for a given breast thickness.

The best way to determine that technique factors are optimized for the detection of low-contrast lesions in digital mammography is to conduct experiments that replicate the clinical situation as closely as possible, using the digital detector of interest. That has been done in this study using phantoms made from tissue-equivalent materials that included simulated low-contrast lesions.

Our results indicate that for a CsI scintillator and amorphous silicon detector, low-contrast lesion detection is maximized by using a softer x-ray beam (relatively low kVp) for thin breasts. Contrast-detail results for digital and screen-film mammography in thin breasts indicate that FFDM should not be expected to yield low-contrast lesion detection superior to that of SFM.

Our results indicate that for 4 cm thick breasts, low-contrast lesion detection was insensitive to the target–filter and kVp selected between 25 and 35 kVp. For thick breasts (>5 cm thick), on the other hand, low-contrast detection is maximized with this detector by selecting a harder x-ray beam. Our results indicated that at 6 cm, Rh–Rh at 30–35 kVp was optimum; at 8 cm, Rh–Rh at 40–46 kVp was optimum. This is due to the combined effect of decreased breast absorption (and therefore decreased breast dose) for higher-energy x rays in thicker breasts and higher SNR per unit dose for higher-energy x rays. The use of a harder x-ray beam for thicker breasts has the added clinical benefit of increasing x-ray output, keeping exposure times short. This has been confirmed in a separate comparison of FFDM to SFM.[16]

Our results can be compared to others that used different techniques to determine optimal beam spectra for digital mammography.[11] For the CsI-silicon diode array detector, Williams *et al.* calculated a FOM that was approximately constant as a function of kVp for all phantom thicknesses and target–filter combinations. Moreover, their FOM showed no distinction among the 3 different target–filter combinations for 3 cm thick breasts. Our results at 2 and 4 cm show no distinction among target–filter combinations, but our 2 cm results suggest a trend toward better low-contrast detection at lower kVp values.

For 7 cm thick breasts, the FOM used by Williams *et al.* indicated a preference for a Rh–Rh target–filter, but no kVp preference. In agreement with their results, our CD results for 8 cm breasts indicate that Rh–Rh is preferable to the other two target–filter combinations. In contrast to their results, our CD results indicate that higher kVp (up to 45 kVp) is preferable for thick breasts.

The SNR calculations of Williams *et al.* suggested that the Mo–Mo target–filter combination and low kVp was preferable for 3 cm thick breasts. Our CD results for 2 cm breasts concur with their results. Their SNR results found no distinction among the three target–filter combinations for thicker (7 cm thick) breasts, while our CD results find a clear preference for the Rh–Rh target–filter combination and higher kVp values for thicker breasts.

Using Monte Carlo techniques to study contrast as a function of dose for different target–filter and kVp combinations, Dance *et al.* determined that only for the thinnest breasts (2 cm thick) does Mo–Mo provide the optimal spectrum for digital mammography. For thicker breasts, Dance *et al.* determined that other target–filter combinations (Mo–Rh, Rh–Rh, Rh–Al, and tungsten–Rh) are preferable in terms of maintaining adequate SNR at a lower dose. Our results, obtained under the condition of constant breast dose for a given thickness, indicate that Mo–Rh and Rh–Rh, with even higher kVp values than those considered by Dance *et al.*, offer better low-contrast detection for breasts thicker than 5 cm.

While in this paper we focus on low-contrast detection, mammography has the additional task of detecting microcalcifications. Would the conclusions of this paper differ if the phantom had consisted entirely of graded microcalcifications? The work of Dance *et al.* suggests that for the task of maintaining an adequate SNR between calcification and background, alternative target–filter combinations producing harder x-ray beams (Mo–Rh, Rh–Rh, Rh–Al, and tungsten–Rh) would still be preferable to Mo–Mo for breasts thicker than 2 cm, although lower tube potentials (28–30 kVp) might yield the best calcification detection. The greater difference in absorption between calcifications and soft tissues at lower kVp, compared to that between fat and glandular tissues, supports this result.

The contrast-detail phantom used in this study has low-contrast targets over a uniform background. This does not fully simulate low-contrast detection in breasts, in that the phantom lacks the additional structured noise caused by fibroglandular tissues. Thus, in the experiments we have performed, the dominant source of noise limiting low-contrast detection was quantum mottle. The difficulty in simulating structured noise in contrast-detail experiments is that, unlike quantum mottle, structured noise is spatially variant. Thus, the results of CD experiments would vary depending on the specific alignment of the CD phantom with the structured noise pattern. To avoid this complication, we have included only quantum mottle noise effects. We believe that our results have clinical relevance, even in the presence of structured noise, as long as quantum mottle is not insignificant in comparison to structured noise.[17]

V. CONCLUSIONS

These results indicate that low-contrast lesion detection is optimized for a CsI silicon diode array detector under the constraint of the fixed breast dose by using a softer x-ray beam for thin breasts and a harder x-ray beam for thick breasts. Under this constraint, FFDM CD scores were superior to SFM CD scores for all but the thinnest breasts.

ACKNOWLEDGMENTS

This work was supported by the Lynn Sage Breast Cancer Research Foundation and by the U.S. Army Medical Research and Material Command Award No. DAMD 17-99-1-9144.

[a]Address all correspondence to Eric A. Berns, Ph.D., The Lynn Sage Comprehensive Breast Center, Northwestern University Medical School, Galter Pavilion, 13th Floor, 251 E. Huron. St., Chicago, Illinois 60611. Telephone: 312-695-3439; fax: 312-926-6224; electronic-mail: eberns@radiology.northwestern.edu

[1]S. W. Fletcher, W. Black, R. Harris, B. K. Rimer, and X. Shapiro, "Report of the international workshop of screening for breast cancer," J. Natl. Cancer Inst. **85**, 1644–1656 (1993).

[2]J. M. Elwood, B. Cox, and A. K. Richardson, "The effectiveness of breast cancer screening by mammography in younger women," Online J. Curr. Clin. Trials **1**, 32–227 (1993).

[3]R. E. Bird, T. W. Wallace, and B. C. Yankaskas, "Analysis of cancers missed at screening mammography," Radiology **184**, 613–617 (1992).

[4]L. Ma, E. Fishell, B. Wright, W. Hanna, S. Allan, and N. F. Boyd, "Case-control study of factors associated with failure to detect breast cancer by mammography," J. Natl. Cancer Inst. **84**, 781–785 (1992).

[5]M. T. Mandelson, N. Oestreicher, P. L. Porter *et al.*, "Breast density as a predictor of mammographic detection: comparison of interval and screen-detected cancers," J. Natl. Cancer Inst. **92**, 1081–1087 (2000).

[6]R. M. Nishsikawa, G. E. Mawdsley, A. Fenster, and M. J. Yaffe, "Scanned-projection digital mammography," Med. Phys. **14**, 717–727 (1987).

[7]R. Fahrig and M. J. Yaffe, "Optimization of spectral shape in digital mammography: dependence on anode material, breast thickness, and lesion type," Med. Phys. **21**, 1473–1481 (1994).

[8]L. E. Court and R. Speller, "A multiparameter optimization of digital mammography," Phys. Med. Biol. **40**, 1841–1861 (1995).

[9]D. R. Dance, A. Thilander-Klang, M. Sandborg *et al.*, "Influence of anode/filter material and tube potential on contrast, signal-to-noise ratio and average absorbed dose in mammography: a Monte Carlo study," Br. J. Radiol. **73**, 1056–1067 (2000).

[10]W. Huda, A. Krol, Z. Jing, and J. M. Boone, "Signal to noise ratio and radiation dose as function of photon energy in mammography," SPIE Med. Imaging **3336**, 355–363 (1998).

[11]M. B. Williams, M. J. More, V. Venkatakkrishnan *et al.*, "Beam optimization for digital mammography," *IWDM 5th International Workshop on Digital Mammography* (Medical Physics, City, 2001), pp. 108–119.

[12]R. E. Hendrick and E. A. Berns, "Optimizing techniques in screen-film mammography," in *Radiologic Clinics of North America: Breast Imaging*, edited by Stephen A. Feig (WB Saunders Co., Philadelphia, 2000), No. 4, pp. 701–718.

[13]X. Wu, E. L. Gingold, G. T. Barnes, and D. M. Tucker, "Normalized average glandular dose in molybdenum target–rhodium filter and rhodium target–rhodium filter mammography," Radiology **193**, 83–89 (1994).

[14]W. T. Sobol and X. Wu, "Parameterization of mammography normalized average glandular dose tables," Med. Phys. **24**, 547–554 (1997).

[15]R. G. Miller, Jr., *Beyond ANOVA, Basics of Applied Statistics* (Wiley, New York, 1986).

[16]R. E. Hendrick and E. A. Berns, "Optimizing mammographic technique," in *1999 Syllabus: Categorical Course in Diagnostic Radiological Physics; Physical Aspects of Breast Imaging—Current and Future Considerations*, edited by A. G. Haus and M. J. Yaffe (Oak Brook, IL, RSNA Publications, pp. 79–89, 1999.

[17]E. A. Berns, R. E. Hendrick, and G. A. Cutter, "Performance comparison of full-field digital mammography to screen-film mammography in clinical practice," Med. Phys. **29**, 830–834 (2002).